JGR Biogeosciences

RESEARCH ARTICLE
10.1029/2024JG008117

Nitrate Loads From Land to Stream Are Balanced by In-Stream Nitrate Uptake Across Seasons in a Dryland Stream Network

Amalia M. Handler[1,2], **Ashley M. Helton**[3], **and Nancy B. Grimm**[1]

[1]School of Life Sciences, Arizona State University, Tempe, AZ, USA, [2]Center for Public Health and Environmental Assessment, Office of Research and Development, U.S. Environmental Protection Agency, Corvallis, OR, USA, [3]Department of Natural Resources and the Environment, and the Center for Environmental Sciences and Engineering, University of Connecticut, Storrs, CT, USA

Key Points:

- Nitrate loading to a dryland stream network varies spatially and seasonally due to hydrologic connection to landscape nutrient sources
- High in-stream nitrate uptake maintained low stream nitrate concentration and watershed export even when landscape inputs were high
- In drylands, hydrologic disconnections in space and time between nitrate sources and the stream requires a flexible modeling approach

Supporting Information:

Supporting Information may be found in the online version of this article.

Correspondence to:

A. M. Handler,
handler.amalia@epa.gov

Citation:

Handler, A. M., Helton, A. M., & Grimm, N. B. (2024). Nitrate loads from land to stream are balanced by in-stream nitrate uptake across seasons in a dryland stream network. *Journal of Geophysical Research: Biogeosciences*, *129*, e2024JG008117. https://doi.org/10.1029/2024JG008117

Received 4 MAR 2024
Accepted 31 OCT 2024

Author Contribution:

Conceptualization: Amalia M. Handler
Data curation: Amalia M. Handler
Formal analysis: Amalia M. Handler
Investigation: Amalia M. Handler
Methodology: Amalia M. Handler
Visualization: Amalia M. Handler
Writing – original draft: Amalia M. Handler
Writing – review & editing: Amalia M. Handler

Abstract Exploring nitrogen dynamics in stream networks is critical for understanding how these systems attenuate nutrient pollution while maintaining ecological productivity. We investigated Oak Creek, a dryland watershed in central Arizona, USA, to elucidate the relationship between terrestrial nitrate (NO_3^-) loading and stream NO_3^- uptake, highlighting the influence of land cover and hydrologic connectivity. We conducted four seasonal synoptic sampling campaigns along the 167-km network combined with stream NO_3^- uptake experiments (in 370–710-m reaches) and integrated the data in a mass-balance model to scale in-stream uptake and estimate NO_3^- loading from landscape to the stream network. Stream NO_3^- concentrations were low throughout the watershed (<5–236 μg N/L) and stream NO_3^- vertical uptake velocity was high (5.5–18.0 mm/min). During the summer dry (June), summer wet (September), and winter dry (November) seasons, the lower mainstem exhibited higher lateral NO_3^- loading (10–51 kg N km^{-2} d^{-1}) than the headwaters and tributaries (<0.001–0.086 kg N km^{-2} d^{-1}), likely owing to differences in irrigation infrastructure and near-stream land cover. In contrast, during the winter wet season (February) lateral NO_3^- loads were higher in the intermittent headwaters and tributaries (0.008–0.479 kg N km^{-2} d^{-1}), which had flowing surface water only in this season. Despite high lateral NO_3^- loading in some locations, in-stream uptake removed >81% of NO_3^- before reaching the watershed outlet. Our findings highlight that high rates of in-stream uptake maintain low nitrogen export at the network scale, even with high fluxes from the landscape and seasonal variation in hydrologic connectivity.

Plain Language Summary Exploring nitrogen dynamics in desert streams is critical for understanding how these systems can reduce pollution while maintaining healthy ecosystems. We examined how seasons and human activities, like farming and development, affect nitrogen pollution in a desert stream in Arizona, USA. We found that in seasons with little rain, nitrogen delivery to the stream was high in areas where irrigation is common. However, in-stream nitrogen remained low because of the high capacity of the stream algal and microbial community to remove nitrogen from the water. This reveals that plants and microbes play a vital role in regulating nitrogen in deserts. This study has broad implications beyond this particular desert stream, emphasizing the importance of understanding complex interactions between human activities, water, and stream microbes. By studying these interactions, we can better manage and preserve desert streams with changing climate and human pressures.

1. Introduction

Nitrogen is an essential nutrient for ecosystem productivity. Biologically available nitrogen enters watersheds through nitrogen fixation and atmospheric deposition as well as human-driven inputs such as fertilizer application and waste (Galloway et al., 2004). As nitrogen moves from hillslope to stream via water transport, the nutrient is subject to transformation and retention (Wollheim et al., 2018). Water mediates not only the transport of nitrogen through the environment, but also the ecosystem productivity responsible for transformation and retention (Belnap et al., 2005; Collins et al., 2014; Noy-Meir, 1973). This is especially the case in drylands, where episodic precipitation coupled with high evapotranspiration leads to variable hydrologic connectivity between land and stream. Streams, having elevated water availability compared to the surrounding landscape, act as hotspots for nitrogen transformation and uptake, relying on inputs from upstream or the surrounding landscape (Bernhardt et al., 2017; Gómez-Gener et al., 2021; Grimm, 1987; von Schiller et al., 2017). As a result, in addition to nitrogen

inputs, hydrologic flowpaths and their variability are critical for understanding nitrogen cycling, especially in drylands.

Stream networks in drylands vary in their capacity for nitrogen cycling in time and space. Temporal variation is driven by the timing of nitrogen inputs to the stream. Stream nitrogen inputs, in turn, are driven partly by the timing of precipitation and partly by the balance of precipitation and evapotranspiration. Precipitation, either sustained inputs during rainy seasons or episodic inputs from individual storms, coupled with evapotranspiration control hydrologic connectivity between land and stream (Bernal et al., 2013; Jencso et al., 2009; Stieglitz et al., 2003). This hydrologic connection is a major pathway for nitrogen transport from upland sources to the stream network; however, biological productivity along transport pathways subjects nitrogen to transformation and retention, exerting an additional control on nitrogen transfers to the stream network (Welter et al., 2005). Indeed, export reflects the balance of transport rates relative to biological reaction rates (Fischer et al., 1998; Ren et al., 2023; Wollheim et al., 2018). Dry conditions lead to lower biological activity and lower connectivity between land and stream. Under these conditions, nitrogen can accumulate on the landscape in the absence of water for transport (Arce et al., 2014).

Spatial variation in dryland stream networks with respect to nitrogen cycling is driven by a combination of natural and human influences. Drylands do not conform to several common assumptions of stream network models (Helton et al., 2011). First, discharge in dryland streams does not necessarily increase with upstream drainage area. Dryland streams often have a preponderance of losing reaches, where groundwater recharge, evapotranspiration, and flow through anthropogenic diversions can substantially decrease streamflow (Alger et al., 2021). While these are common water-loss pathways in any watershed, in dryland systems these fluxes can be a substantial proportion of, or even greatly exceed, surface flow (Goodrich et al., 2018). Second, dryland ecosystems challenge the assumption that surface flows converge in the downstream direction, often having diverging flowpaths, for example, due to irrigation diversions. In some systems, these diversions can account for the entire main-channel flow (Hill & Walter, 2020). Depending on water demand for irrigation, some water may be returned to the main channel at a downstream location or it may be entirely consumed.

While models commonly estimate nitrogen concentration in streams based on factors such as point sources, land use, and land cover (Preston et al., 2011), the highly variable hydrologic connections between nitrate (NO_3^-) sources and streams leave room for substantial temporal disconnections between nitrogen inputs to the landscape and transport to streams (Welter et al., 2005). In dryland streams, NO_3^- is the predominant form of biologically available nitrogen (Grimm & Fisher, 1986). Dryland streams are generally nitrogen-limited with high uptake rates relative to other ecosystem types (Grimm & Fisher, 1986; Grimm & Petrone, 1997; Hall et al., 2009; Martí & Sabater, 1996). Therefore, the interplay between stream NO_3^- uptake and NO_3^- loading from the landscape adds further complexity, particularly in dryland contexts where in-stream uptake holds potential to substantially attenuate nitrogen concentration relative to inputs (Bernal et al., 2013). Failure to represent spatial and temporal variations in hydrology and the influence of stream NO_3^- uptake hampers the study of nutrient dynamics in dryland streams, particularly at the network scale (Helton et al., 2011).

The goal of this study is to evaluate how in-stream NO_3^- concentration, in-stream NO_3^- uptake, and NO_3^- loading from the land to streams vary spatially and seasonally along a dryland stream network. To achieve this goal, we (a) measured and compared stream NO_3^- concentration, stream flow, and in-stream NO_3^- uptake among seasons and stream sizes (tributaries and ditches vs. mainstem), (b) integrated these data in a mass-balance model that explicitly incorporates hydrologic dynamics (groundwater recharge and flow diversions) critical for modeling nitrogen dynamics in dryland streams to scale in-stream NO_3^- uptake to the whole river network, (c) evaluated spatial and temporal patterns of modeled lateral NO_3^- loading, in-stream NO_3^- uptake, and their relationships with each other and land cover across the stream network. We hypothesized that high in-stream NO_3^- uptake (as is typical from dryland systems) would result in low stream NO_3^- load at the Oak Creek outlet and high stream network NO_3^- uptake during drier seasons with lower landscape to stream hydrologic connectivity. During seasons with higher hydrologic connectivity (higher precipitation), we hypothesized there would be higher lateral NO_3^- loads to the stream that would eventually exceed in-stream NO_3^- uptake capacity, resulting in higher NO_3^- loads at the Oak Creek outlet.

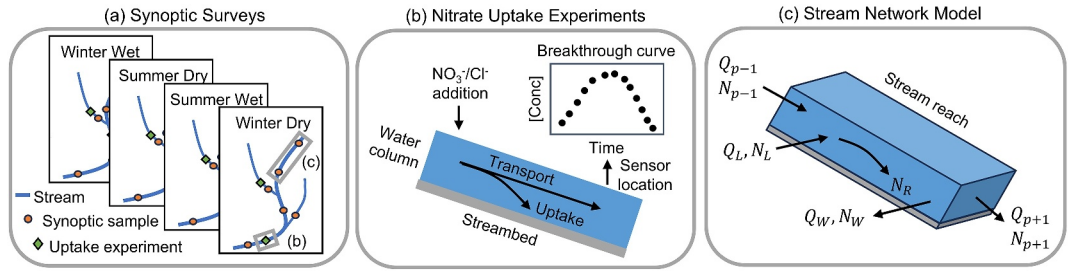

Figure 1. Schematic diagram of (a) the seasonal synoptic surveys (Section 2.2), (b) stream NO_3^- uptake experiments (Section 2.3), and (c) stream network model (Section 2.4).

2. Materials and Methods

2.1. Site Description

Oak Creek is a tributary of the Verde River in the transition zone between the Basin and Range Province and the Colorado Plateau in Arizona, U.S. The creek originates at an elevation of 2,300 m in ponderosa pine forest and descends through pinyon-juniper and high desert ecosystems to its confluence with the Verde River at 950 m elevation. Central Arizona has two rainy seasons separated by two dry seasons. The winter-spring rainy season (January–April) is characterized by frontal systems dominating precipitation in the form of rain and snow. The dry summer season (May–July) can feature daytime high temperatures that regularly exceed 36°C. The summer rainy season (August–September) is characterized by convective monsoon storms. The post-summer rainy season (October–December) is a dry period characterized by lower temperature and less rainfall. Rainfall amounts and timing in both rainy seasons exhibit high interannual variability.

Oak Creek drains a 1,200 km^2 watershed. The main stem of Oak Creek is perennial, as are short sections of three spring-fed tributaries. The remainder of the network is temporary (including intermittent and ephemeral streams), with some channels having seasonal surface water and many others supporting surface flow only during large storms. The Oak Creek main stem and perennial tributaries are bordered by a riparian gallery forest of cottonwood and willow; however, the stream channel's canopy is open except for the smallest, high-elevation tributaries (most of which are not perennial).

Land cover in the watershed is mostly undeveloped (>95%), with some green space, residential, and commercial developed area (4%) around the cities of Sedona and Cornville and a small proportion of agricultural cover (<1%). There are two fish hatcheries in the watershed that rely on springs for water supply and discharge water to the main channel of Oak Creek (Oak Creek Watershed Council, 2012). Residential and agricultural areas are irrigated through a combination of diverted stream water and groundwater wells.

To test our hypothesis that seasonal differences in precipitation increases hydrologic connectivity that would change the balance of lateral NO_3^- loading and in-stream NO_3^- uptake at the network scale, we conducted synoptic surveys coupled with NO_3^- uptake experiments (Figure 1). We then integrated these data in a mass-balance model to scale in-stream NO_3^- uptake to the entire stream network.

2.2. Synoptic Sampling

We conducted four seasonal sampling campaigns of stream water chemistry and discharge across Oak Creek. Campaigns took place in 2017 during the winter wet season (February; minimum and maximum air temperature for sample dates: 0 and 11°C), summer dry season (June; 20 and 36°C), summer wet season (September; 15 and 29°C), and winter dry season (November; 10 and 23°C; Figure 2). During each campaign, we sampled 25–29 sites distributed across the watershed. Sites along the main stem were selected to target locations above and below confluences and irrigation divisions, and otherwise were evenly spaced. Both perennial and intermittent (when flowing) tributaries as well as irrigation ditches were sampled. Often, only one site along an irrigation ditch was accessible. We identified and sampled two sites that drain fish hatcheries, and noted a trout farm adjacent to the main stem of Oak Creek in the upper portion of the watershed. The main stem sites included locations below these potential point sources. Most sites were accessed via public lands with a small subset accessed via private land with permission. The campaign during the winter wet season was the first completed and took place during a

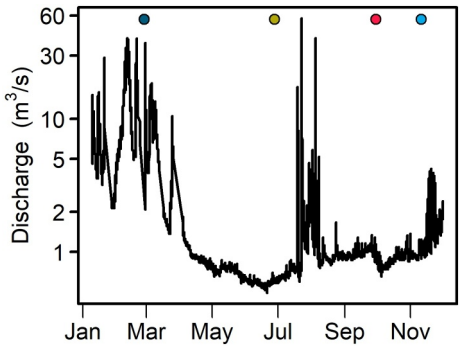

Figure 2. Discharge on the main stem of Oak Creek (USGS Gage: 09504500). Dots indicate when each synoptic sampling campaign took place.

period of high discharge relative to the latter campaigns. As a result, many sampling locations were difficult or impossible to access during this season. Subsequent campaigns were adjusted and thus there are fewer sampling sites in the winter wet season in common with those collected in the latter seasons.

To estimate stream discharge and surface area, we measured stream wetted width and recorded 10–15 depth measurements at regular width intervals at each site. We calculated cross-sectional area by summing the area bounded by each depth measurement. For the main channel, tributaries, and larger irrigation ditches, we measured water velocity at each depth measurement. We calculated discharge as the cross-sectional area times the mean water velocity. For smaller irrigation ditches, we used pulse injection of sodium chloride (NaCl) to measure discharge via dilution gauging (Day & Day, 1977).

At each site, we collected duplicate, field-filtered water samples (0.7 μm GFF syringe filter, Fisher Scientific) for analysis of NO_3^-, ammonium (NH_4^+), and chloride (Cl^-). Chloride is a non-biologically reactive ion that can indicate a change in water source. Samples were stored in a cooler on dry ice until returned to the lab where samples were stored at −20°C until analysis. Nitrate (NO_3^- plus NO_2^-; hereafter NO_3^- in units of μg N/L), NH_4^+ (μg N/L), and Cl^- (mg/L) concentrations were analyzed via Lachat QC 8000 flow injection analyzer (Lachat Instruments, Loveland, CO). Ammonium was uniformly low across seasons with approximately 20% of samples below the detection limit (10 μg N/L) and 80% of samples below 20 μg N/L. As a result, NH_4^+ will not be discussed further.

2.3. Nitrate Uptake Experiments

To determine the NO_3^- uptake rate in Oak Creek and tributaries, we conducted seasonal nutrient-spiraling experiments to pair with the sampling campaigns (Newbold et al., 1981). We conducted a total of nine experiments by pulse injection (Covino et al., 2010). The experiments were conducted once per season on the main stem of Oak Creek in 2017 in the spring (April), summer dry season (June), summer rainy season (September), and winter dry season (November). Discharge in the main stem was prohibitively high earlier in the winter wet season (February and March) and only dropped to a level that allowed the experiment in April. Experiments also took place once per season in the perennial tributary Spring Creek in the winter wet, summer dry, summer wet, and winter dry seasons. An additional experiment was conducted in Dry Creek, an intermittent tributary, in the winter wet season. The winter wet season was the only period for which Dry Creek had flowing surface water during 2017.

Each experiment was conducted by dissolving NaCl (conservative tracer) and sodium nitrate ($NaNO_3$, reactive tracer) into 10–50 L of stream water collected from the site. The mass of NaCl and $NaNO_3$ were adjusted such that the solution would raise the NO_3^- concentration by 50 μg N/L and chloride by 6.5 mg/L at the downstream collection location when added in a single pulse. The reach lengths from the injection point to the collection point were 710, 400, and 370 m for Oak, Spring, and Dry Creeks, respectively. Reach lengths were determined during pre-experiment tests to ensure that both tracers had fully mixed across the stream width and depth. Following collection of background water samples, the tracer-enriched water was added to the stream instantaneously. Monitoring at the collection location took place with an electrical conductivity meter (either YSI 556 MPS, YSI 600 XLM, YSI DSM Pro, or Eureka Manta) and a SUNA NO_3^- sensor (Sea-Bird Scientific, Bellevue, WA). The SUNA is factory calibrated by Sea-Bird Scientific. For the Dry Creek experiment, due to SUNA instrument failure, we instead collected 23 grab samples distributed across the breakthrough curve at the collection location for analysis of NO_3^-. An injection was considered complete when electrical conductivity had returned to within 1 μS/cm of the background measurement or more than 3 hr had elapsed since the injection time. In cases where experiment were concluded after the full 3 hr, electrical conductivity was 2–3 μS/cm above the pre-experiment background. All grab samples were collected in duplicate in 500-mL HPDE Nalgene® bottles; subsamples were poured into 50-mL centrifuge tubes for transport to the lab on ice and stored at −20°C until analysis as described above.

Data from the experiments were processed using the TASCC method described by Covino et al. (2010). Briefly, electrical conductivity together with NO_3^- data were background-corrected, and interpolated to 1-min intervals over the breakthrough curve. The breakthrough curve was adjusted to have an equal number of observations for

the rising and falling limbs of the curve. The first-order uptake-rate coefficient was calculated by taking the log of the background-corrected ratio of NO_3^-:Cl^- of each observation divided by the same ratio in the injection solution all divided by the distance between the injection and collection points. Uptake length (S_w) was calculated for each observation by taking the inverse of the uptake coefficient. A regression between S_w and the associated NO_3^- concentration was used to estimate S_w for the stream at the background NO_3^- concentration by extrapolation. Either a first-order (linear) or loss of efficiency (log-transformed) regression was used according to O'Brien et al. (2007), including estimation of 95% confidence intervals for the uptake parameters at the background NO_3^- concentration. The vertical uptake velocity (v_f) was calculated by multiplying the inverse of S_w by the reach discharge and dividing by the mean reach width. We used a travel-time correction to control for the differing amounts of time each sample had in the stream prior to collection (Covino et al., 2010).

2.4. Stream Network Model

We used a steady-state mass-balance model to combine the field measured in-stream NO_3^- concentrations and NO_3^- uptake rates at the network scale in order to evaluate how much in-stream uptake attenuates lateral NO_3^- loads (Helton et al., 2011; Mulholland et al., 2008). Following Helton et al. (2011), we implemented the model using an inverse approach to estimate patterns of lateral NO_3^- loading from land to stream reaches. The model estimates the lateral NO_3^- load necessary to reproduce the observed spatial patterns in stream NO_3^- load, given the field-based stream NO_3^- uptake rate, discharge, and stream NO_3^- concentration. The model accounts for both serial processing of NO_3^- along the network and water diversions.

Discharge (Q, in volume/time) for each reach was calculated by subtracting outgoing water from incoming water according to the following equations

$$Q_p = \left(\sum Q_{p-1_i} + Q_L\right) - (Q_W + Q_{p+1_i}) \quad (1)$$

where

$$Q_L = A_p \times Y_p \quad (2)$$

where Q_p is the discharge in-stream reach p, $\sum Q_{p-1_i}$ is the sum of the discharge of upstream reaches, $p-1_i$, contributing discharge to stream reach p, Q_L is the lateral discharge from the adjacent drainage area, Q_W is water loss from reach p, Q_{p+1} is the discharge to the next downstream reaches $p+1_i$, A_p is the area of the catchment draining directly to stream reach p, and Y_p is the per unit subcatchment area lateral water yield to stream reach p. We modified the existing model to include the term Q_W, which represents the sum of water loss to diversion or groundwater recharge.

For flowing reaches, we parameterized the lateral water yield (Y_p in Equation 2) for each season and stream segment based on the discharge measured during the respective synoptic sampling campaign. The change in discharge for each reach was calculated as the discharge at the reach outlet minus the sum of discharge from the upstream reach and any tributary confluences and irrigation returns. Generally, only one site was accessible along irrigation ditches and we assumed discharge to be uniform along their length for the model. For network reaches containing an irrigation diversion, the discharge in the ditch was subtracted from the main channel. Each season included both net gaining and net losing stream reaches. We parameterized lateral water yield as a gross process where each stream reach has both lateral water input and loss. Lateral water yield was calculated by dividing the change in discharge by the lateral drainage area to the reach (Equation 2). We implemented this by applying a lateral water yield to each subcatchment that would produce the maximum discharge measured in each season. From this, we calculated a stream water loss term (Q_W in Equation 1) necessary to produce the field-measured discharge. Water loss encompasses stream water transfer to the hyporheic zone and groundwater (Lange, 2005; Valett et al., 1994), mechanical withdrawal to supply potable or irrigation water (Alger et al., 2021), and evapotranspiration (Dahm & Molles, 1992). By implementing the lateral water flows as a gross rather than net process, we allow for lateral inputs of NO_3^- to stream reaches that have net discharge loss.

Stream NO_3^- load (N, in mass/time) is modeled similarly by subtracting the outgoing NO_3^- load from incoming load

$$N_p = \left(\sum N_{p-1_i} + N_L\right) - (N_R + N_W + N_{p+1_i}) \quad (3)$$

where

$$N_L = A_p \times L_p \quad (4)$$

where N_p is the NO_3^- load in stream reach p, $\sum N_{p-1_i}$ is the sum the of NO_3^- load from all upstream reaches contributing NO_3^- to stream reach p, N_L is the lateral NO_3^- load from the adjacent drainage area, N_R is the stream NO_3^- load taken up from reach p, N_W is NO_3^- loss due to water loss from the reach, N_{p+1_i} is the stream NO_3^- load to the next downstream reach $p+1$, A_p is the area of the catchment draining directly to stream reach p, and L_p is the lateral NO_3^- load per unit drainage area to stream reach p. Nitrate loss stemming from water loss (N_W) is calculated by multiplying the water loss by the NO_3^- concentration in stream reach p. Lateral NO_3^- load per unit drainage area is the primary model term of interest in this analysis. Negative lateral NO_3^- loading (L_p) signifies that there was not sufficient uptake capacity in a stream reach or not a sufficient decrease from water loss to achieve the measured NO_3^- concentration (i.e., that NO_3^- concentration was lower than would be predicted based on upstream concentration and uptake rate). For each stream reach, the mass of NO_3^- removed (N_R, in mass/time) is equal to the total NO_3^- load in the stream reach times the fractional removal factor

$$N_R = R \times N_p \quad (5)$$

The fractional removal factor is determined according to the following equation from Wollheim et al. (2006).

$$R = 1 - e^{(-v_f/H_L)} \quad (6)$$

where

$$H_L = Q_p/SA_p \quad (7)$$

and v_f is the experimentally determined vertical uptake rate for NO_3^- (in length/time).

We parameterized in-stream NO_3^- uptake in the model based on field data. The vertical uptake rate (v_f in Equation 6) was determined based on the median of all stream NO_3^- uptake rates measured in the main channel and tributaries (Section 2.3) since v_f did not vary significantly based on season or stream type. Initial model testing with the minimum and maximum NO_3^- uptake values measured experimentally changed only the magnitude of the lateral NO_3^- load, but patterns and overall stream network NO_3^- attenuation remained high. The v_f is normalized by hydraulic load (H_L in length/time), which is a measure of the rate of water passage through the stream relative to the benthic surface area. Hydraulic load is calculated by dividing the discharge (Q_p in volume/time) by the surface area (SA_p, calculated as stream length times average width). Average stream width (w) is estimated as

$$w = aQ^b \quad (8)$$

where a and b are the width coefficient, which controls the scaling, and width exponent, which controls the rate of increase, respectively (Leopold & Maddock, 1953). Both a and b were determined from field survey data from each season (Table S1 in Supporting Information S1).

We implemented four steady-state models, one for each synoptic sampling campaign that represents the dynamics of each season: Winter wet, summer dry, summer wet, and winter dry. We derived network structure from the National Hydrography Data set Plus Version 2 (NHDPlusV2) flowlines, flow direction, and drainage area. This included the two largest irrigation ditches in the watershed that have both diversions from and returns to the main channel of Oak Creek. We derived subcatchments for each synoptic sampling location for each season by delineating the drainage area for each reach between sampling locations. Reaches were further subdivided into

segments between network junctions (e.g., tributary confluences, irrigation diversions, irrigation returns) or 1,000 m, whichever was shorter.

The extent of the flowing portion of the drainage network varied between campaigns. For the summer dry, summer wet, and winter dry seasons, the extent of the flowing network followed the perennial flow designations in the NHDPlusV2. For the winter wet season, one large tributary and two headwater streams had flowing surface water that were coded as intermittent or ephemeral in the NHDPlusV2. Across surveys, flowlines that did not have flowing surface water were parameterized to have negligible lateral water yield. We estimated lateral NO_3^- loading (L_p) by using a model-independent parameter estimator (PEST 16.0, Model-Independent Parameter Estimation & Uncertainty Analysis). PEST adjusts model parameters, based on their values and model outputs, compared to observed data. In this instance, PEST was used to adjust the lateral NO_3^- loads to reproduce the measured in-stream NO_3^- load observed at each sampling location. The lateral NO_3^- loads lack error estimates because these would be based largely on error associated with the in-stream NO_3^- uptake. Initial model testing revealed that varying the stream NO_3^- uptake changed only the magnitude of the lateral NO_3^- load, but patterns in lateral NO_3^- load and overall stream network NO_3^- attenuation remained similar.

2.5. Land-Cover Data

To test whether lateral NO_3^- loads are associated with land cover, we used the 2011 National Land Cover Database (NLCD) (Dewitz, 2014). We calculated zonal statistics for land-cover types at two scales: (a) The subcatchment area and (b) a 200-m buffer area extending perpendicular to the direction of flow (100 m on both sides of the stream). For each subcatchment and buffer area, we calculated the proportions of total agricultural land (sum of NLCD cropland and hay/pasture), developed land (sum of NLCD developed open spaces and low-, medium-, and high-intensity development), and wetland area (sum of NLCD herbaceous and woody wetlands). The 2011 NLCD was the best available data at the time of the analysis; however, we reviewed changes in the percent cover of the classes included in this study between the 2011 and 2016 NLCD and found that most changes were negligible to small (<2.5%).

2.6. Data Analysis

We evaluated seasonal differences and spatial patterns within Oak Creek watershed using the measured discharge, stream NO_3^- and Cl^- concentrations, NO_3^- uptake experiments, and hydrologic and lateral NO_3^- loading model outputs. We evaluated the fluvial network patterns in stream discharge, NO_3^- concentration, and Cl^- concentration by plotting the data against distance from the watershed outlet, and plotted the lateral NO_3^- loads in map format. Nitrate and Cl^- concentration measurements below the detection limit were replaced with a value one half of the detection limit for visualization and statistical analysis. We tested for seasonal differences in discharge, chemistry, NO_3^- uptake, and lateral NO_3^- loads using a one-way analysis of variance (ANOVA). In addition, we tested for differences in-stream chemistry among site types (i.e., main channel, tributary, irrigation ditch) using ANOVA. We varied the base group in the ANOVA to evaluate pairwise differences between groups. We evaluated the ratio of NO_3^- to Cl^- to identify outliers that may indicate a difference in source water. We evaluated differences in spatial patterns of discharge and NO_3^- and Cl^- concentrations from the synoptic campaigns by calculating Spearman's correlation coefficient between data for the same sampling locations in different seasons, as a measure of synchrony. We expected that seasons would either (a) have a similar spatial pattern in sources and sinks for discharge, NO_3^- concentration, and Cl^- concentration and therefore exhibit synchrony (i.e., positive pairwise correlations between seasons) or (b) would have a different pattern and thus be asynchronous (i.e., negative or no pairwise correlation between seasons), potentially indicating a different set of sources and sinks. An assumption of this analysis is that the NO_3^- and Cl^- concentrations in the sources do not change much across seasons, which is supported based on findings from another desert stream showing consistency of source chemistry across seasons (Dent & Grimm, 1999) and years (Dong et al., 2017). We completed a similar correlation analysis for the lateral NO_3^- loads from the model, but applied an additional constraint that the subcatchment area needed to cover identical areas among seasons for pairwise comparison. In both correlation analyses, the number of sites included differed in each pairwise comparison because the sample locations differed between the campaigns. In particular, the winter wet season took place during a period with high discharge, making sampling difficult or impossible in many locations. As a result, the winter wet season had comparatively fewer sites and subcatchments that matched the summer dry, summer wet, and winter dry seasons. Finally, we evaluated the relationship between lateral NO_3^- loading and land cover variables as well as stream characteristics

Table 1
Characteristics and Results of the Synoptic Sampling in Oak Creek, Arizona, USA

Season	Sites sampled	Flowing contributing area (km^2)	Flowing stream length (km)	Outlet discharge (m^3/s)	Outlet [NO_3^-] (μg N/L)	Modeled sub-catchments	Sub-catchments net losing discharge
Winter Wet	25	279 (23%)	167	5.42	ND	21	7 (33%)
Summer Dry	29	196 (16%)	111	1.20	8.0	19	5 (26%)
Summer Wet	27	181 (15%)	111	2.12	24.6	20	9 (45%)
Winter Dry	27	182 (15%)	111	2.51	7.1	19	6 (32%)

Note. For each season, the total number of sites sampled, contributing area and parenthetical proportion of the total watershed (area = 1,200 km^2) that was draining to flowing surface water, total stream length with flowing surface water, watershed outlet discharge, watershed outlet NO_3^- concentration (ND = non-detect), the number of modeled subcatchments for each season, and the number (%) of subcatchments that were net losing discharge.

(e.g., discharge, width, depth, and chemistry) using correlation analysis. Correlations with land-cover variables were evaluated at the subcatchment scale and for a 200-m buffer area centered on the stream channel. We evaluated the correlations at these two scales because the subcatchments could be very large, and land cover several kilometers from the stream may be hydrologically disconnected from the stream channel.

In all cases, correlations were calculated using Spearman's rank correlation coefficient (rho) because of non-linear relationships among variables. For correlations between NO_3^- loading and land cover variables, we excluded sites that we suspected were influenced by point sources of nutrients, including the two fish hatcheries and one trout farm. At these locations, we reasoned that NO_3^- loading would be influenced more by the point source than the land cover variables included in the analysis. All statistical analyses were performed in R version 4.3.2 (2023-10-31 ucrt) (R Core Team, 2023).

3. Results

3.1. Patterns of Stream Discharge

The extent of the watershed with flowing surface water was highest in the winter wet season due to several flowing tributaries and headwaters (Table 1). These areas lacked surface water in summer dry, summer wet, and winter dry seasons. As a proportion of the total area in Oak Creek watershed, the catchment area draining to flowing surface water in the winter wet season was 23%, compared to 15%–16% in the other seasons. Discharge in the main stem of Oak Creek ranged from 0.145 m^3/s near the headwaters to 5.55 m^3/s near the watershed outlet and was variable along the length of the main stem (Figure 3). Based on the discharge measurements, 25%–45% of reaches were net losing reaches, meaning that the discharge measured at the downstream location was lower than the sum of all upstream sites (main channel, tributaries, and irrigation returns) draining to that location. The summer wet season had the most losing reaches ($N = 9$ of 20) while the summer dry season had the fewest ($N = 5$ of 19). The summer dry season also had the lowest measured discharge loss across all losing reaches (2.2 m^3/s) while the winter wet season had the highest loss (9.1 m^3/s). There were seasonal differences in mean discharge for the main channel (ANOVA: $F_{(3, 51)} = 10.70$, $p < 0.001$). The winter wet season had significantly higher mean discharge (mean ± standard deviation: 3.1 ± 2.0 m^3/s) than the summer dry (0.7 ± 0.4 m^3/s), summer wet (1.4 ± 0.8 m^3/s), and winter dry (1.5 ± 1.0 m^3/s) seasons.

3.2. Patterns of Stream Chemistry

Nitrate concentration varied from below the detection limit (5 μg N/L) to 236 μg N/L (Figure 3). Chloride varied from below detection (<2.5 mg/L) to 36.7 mg/L. Longitudinal patterns in stream chemistry were similar in the summer dry, summer wet, and winter dry seasons and contrasted with those of the winter wet season. In the summer dry, summer wet, and winter dry seasons, chloride was elevated in the lower (0–25 km from outlet) section of the watershed compared to the upper section. In contrast, the winter wet season had lower chloride in the lower section of the watershed but was elevated in the upper section relative to the three other seasons. Concentration of NO_3^- was positively correlated between paired sampling sites (i.e., was synchronous) in the

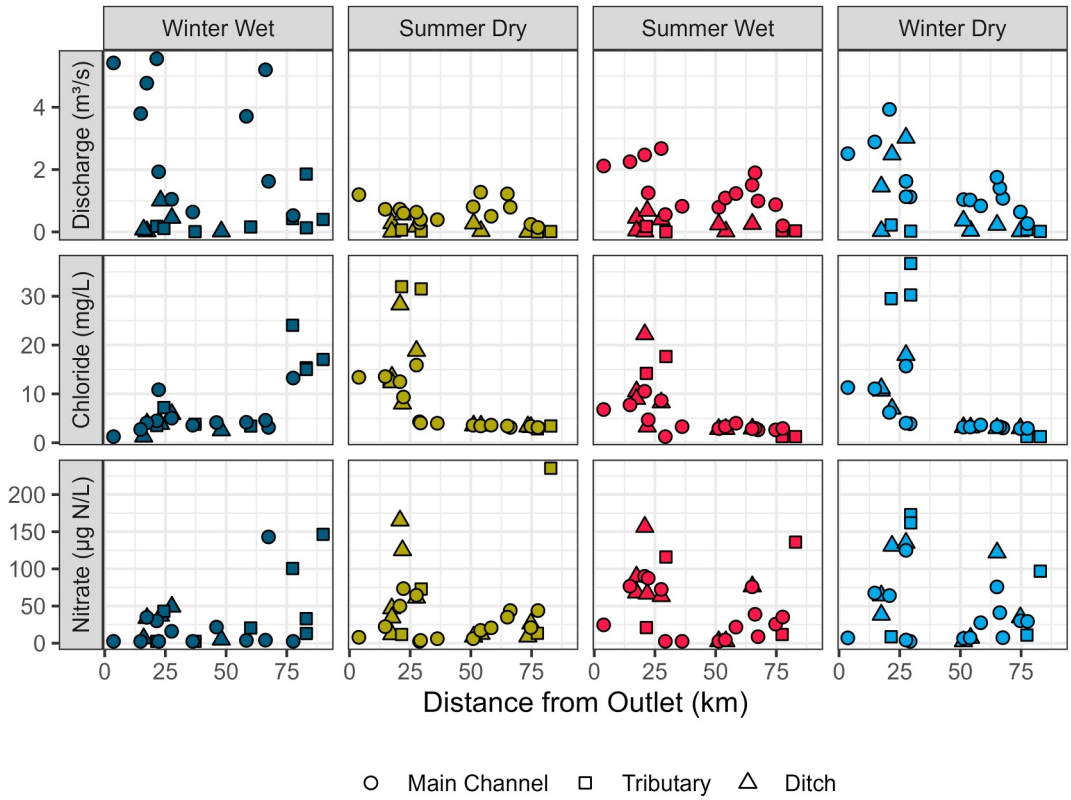

Figure 3. Synoptic survey-measured stream discharge (top row), Cl^- concentration (middle row), and NO_3^- concentration (bottom row) for each season plotted against distance from the watershed outlet (headwaters are to the right in each plot).

summer dry, summer wet, and winter dry seasons (Table 2). Similarly, concentration of Cl^- exhibited synchrony for summer dry, summer wet, and winter dry campaigns. The winter wet season NO_3^- concentration was uncorrelated with those of the summer dry, summer wet, and winter dry seasons. Concentration of Cl^- in the winter wet season was negatively correlated with the winter dry season and uncorrelated with the summer dry and summer wet season (i.e., was asynchronous). Mean Cl^- concentration differed significantly based on site type (ANOVA: $F_{(2,105)} = 11.08$, $p < 0.001$), with highest concentration in tributaries (13.9 ± 12.3 mg/L), followed by irrigation ditches (7.9 ± 6.7 mg/L), and lowest in the main channel (5.5 ± 3.8 mg/L). Mean NO_3^- concentration did not vary significantly by site type. Some sampling locations had exceptionally high NO_3^-/Cl^- ratios relative to the mean of 0.009 (Figure S1 in Supporting Information S1).

3.3. Stream NO_3^- Uptake

Stream NO_3^- uptake length (S_w) varied from a minimum of 219 m (95% confidence interval: 183–255 m) in Dry Creek in the winter wet seasons to a maximum of 575 m (548–602 m) in Oak Creek in spring (April, Figure 4). Stream NO_3^- vertical uptake velocity (v_f) varied from a minimum of 5.5 mm/min (4.7–6.6 mm/min) in Spring Creek in the summer dry season to a maximum of 18.0 mm/min (15.5–21.6 mm/min) in Oak Creek in the winter dry season. Neither of the uptake parameters was correlated with background NO_3^- concentration (S_w rho = 0.65, $p > 0.05$; v_f rho = 0.28, $p > 0.05$) nor was there a systematic difference in uptake between the main channel and tributaries (ANOVA: S_w $F_{(1,7)} = 5.08$, $p > 0.05$; v_f $F_{(1,7)} = 4.82$, $p > 0.05$). The median v_f of 12.3 mm/min was used as the uptake rate parameter for the model.

3.4. Model Results

Integrating across Oak Creek watershed, in-stream NO_3^- uptake removed >98% of lateral NO_3^- inputs in all seasons before streamflow exited the watershed (Table 3). More than 81% of the lateral NO_3^- load was removed by in-stream NO_3^- uptake across searons. Total lateral NO_3^- load ranged from 157 kg N/d in the winter dry

Table 2
Synchrony in Chemistry and Loads Across Seasons

Season	Winter wet	Summer dry	Summer wet	Winter dry
Stream NO_3^- Concentration				
Winter Wet	+1			
Summer Dry	−0.16 (14)	+1		
Summer Wet	+0.15 (13)	+0.86 (24)**	+1	
Winter Dry	+0.15 (13)	+0.85 (25)**	+0.91 (23)**	+1
Stream Cl^- Concentration				
Winter Wet	+1			
Summer Dry	−0.46 (14)	+1		
Summer Wet	−0.48 (13)	+0.84 (24)**	+1	
Winter Dry	−0.59 (13)*	+0.85 (25)**	+0.93 (23)**	+1
Lateral NO_3^- Load				
Winter Wet	+1			
Summer Dry	+0.93 (7)*	+1		
Summer Wet	+0.50 (7)	+0.71 (16)*	+1	
Winter Dry	+0.60 (6)	+0.87 (12)*	+0.95 (13)**	+1

Note. Spearman rank correlation matrix of measured stream NO_3^- and Cl^- concentration, as well as modeled lateral NO_3^- loads across seasons. Values are Spearman's rho with the number of paired observations in parentheses. Asterisks denote a significant correlations (*$p < 0.05$; **$p < 0.001$), indicating synchrony. Pairwise correlations were computed for sites that were sampled in each season for stream NO_3^- and Cl^- concentration. For lateral NO_3^- loads, pairwise correlations were computed for subcatchments that cover identical areas among seasons.

season to 673 kg N/d the summer wet season. At the watershed outlet, combining discharge with the measured NO_3^- concentration yielded stream NO_3^- export ranging from 0.8 kg N/d in the summer dry season to 4.5 kg N/d in summer wet season.

Modeled lateral NO_3^- loading was variable across the network, spanning seven orders of magnitude, including negative and positive values (−1.25 to 51.33 kg N km^{-2} d^{-1}; Figure 5). In total there were six negative lateral NO_3^- loading values (−1.25 to $-2.88 \cdot 10^{-4}$ kg N km^{-2} d^{-1}); all but one of them occurred on the main stem and four of six occurred during the winter wet season. The mainstem had substantially higher lateral NO_3^- loading during the summer wet season, but in general lateral NO_3^- loading varied widely within seasons and was not statistically different among seasons (ANOVA: $F_{(3,75)} = 1$, $p > 0.05$). However, lateral NO_3^- loading was positively correlated among the summer dry, summer wet, and winter dry seasons (i.e., was synchronous; Table 2). Lateral NO_3^- loading in the winter wet season was positively correlated with the summer dry season (rho = 0.93, $p < 0.05$), but no relationship in lateral NO_3^- loading was detected between the winter wet, summer wet, or winter dry seasons.

There were 11 total observations near three suspected point sources of nutrient inputs due to the fish hatcheries and fish farm. These locations had among the highest measured NO_3^- concentrations and NO_3^-/Cl^- ratios. The modeled lateral NO_3^- loading ranged from 0.02 to 5.58 kg N km^{-2} d^{-1} (med = 0.16 kg N km^{-2} d^{-1}) for the subcatchments adjacent to these point sources. Since these locations were presumed influenced by a point source of nutrients, these observations were excluded from the correlation analysis with land cover variables.

3.5. Land Cover and Lateral NO_3^- Loading

Agriculture accounted for a small proportion of land cover at the subcatchment scale (median = 0%–7%; Table S2 in Supporting Information S1). Depending on the season and area evaluated, 4–11 subcatchments of the 16–19 included in the land cover analysis lacked agricultural land cover. At the subcatchment scale, developed area accounted for a similar proportion of

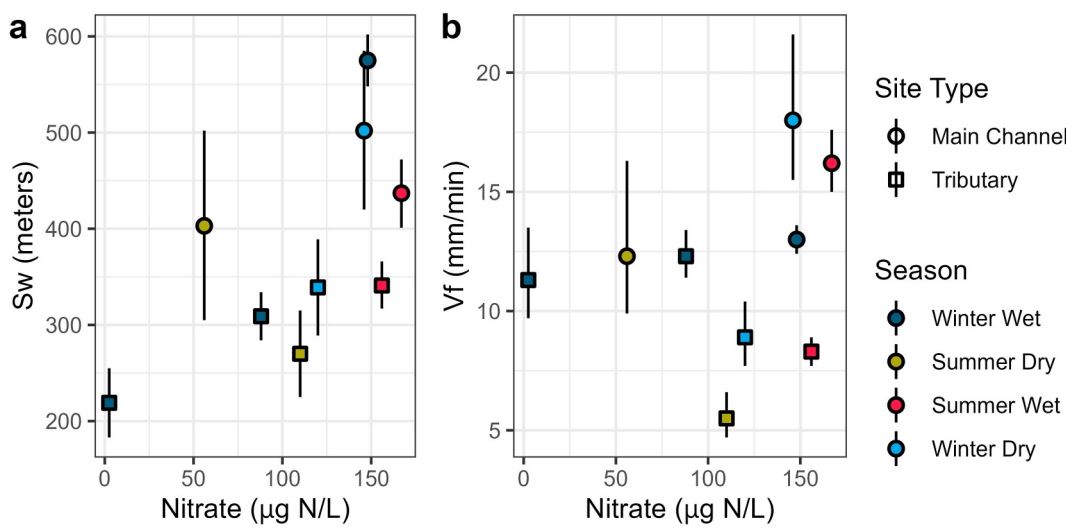

Figure 4. Stream NO_3^- uptake length (S_w; a) and vertical uptake velocity (v_f; b) estimated for the background NO_3^- concentration at the time of the experiment in the main channel and tributaries of Oak Creek. Points are colored according to the season that the experiment took place. Error bars represent the 95% confidence intervals for the uptake parameters.

Table 3
The Total Watershed Lateral NO_3^- Load and Fate of NO_3^- as Export at the Stream Outlet, Output Along the Stream Network From Water Loss, and Removal by In-Stream Uptake

Season	Total lateral NO_3^- load (kg N/d)	Stream outlet NO_3^- load (kg N/d)	Total NO_3^- loss via water loss (kg N/d)	Total in-stream NO_3^- removal (kg N/day)
Winter Wet	187.4	1.2 (0.6%)	28.3 (15.1%)	157.9 (84.3%)
Summer Dry	274.7	0.8 (0.3%)	0.9 (0.3%)	272.0 (99.4%)
Summer Wet	673.0	4.5 (0.7%)	28.1 (4.2%)	640.4 (95.1%)
Winter Dry	157.2	1.5 (1.0%)	27.1 (17.2%)	128.6 (81.8%)

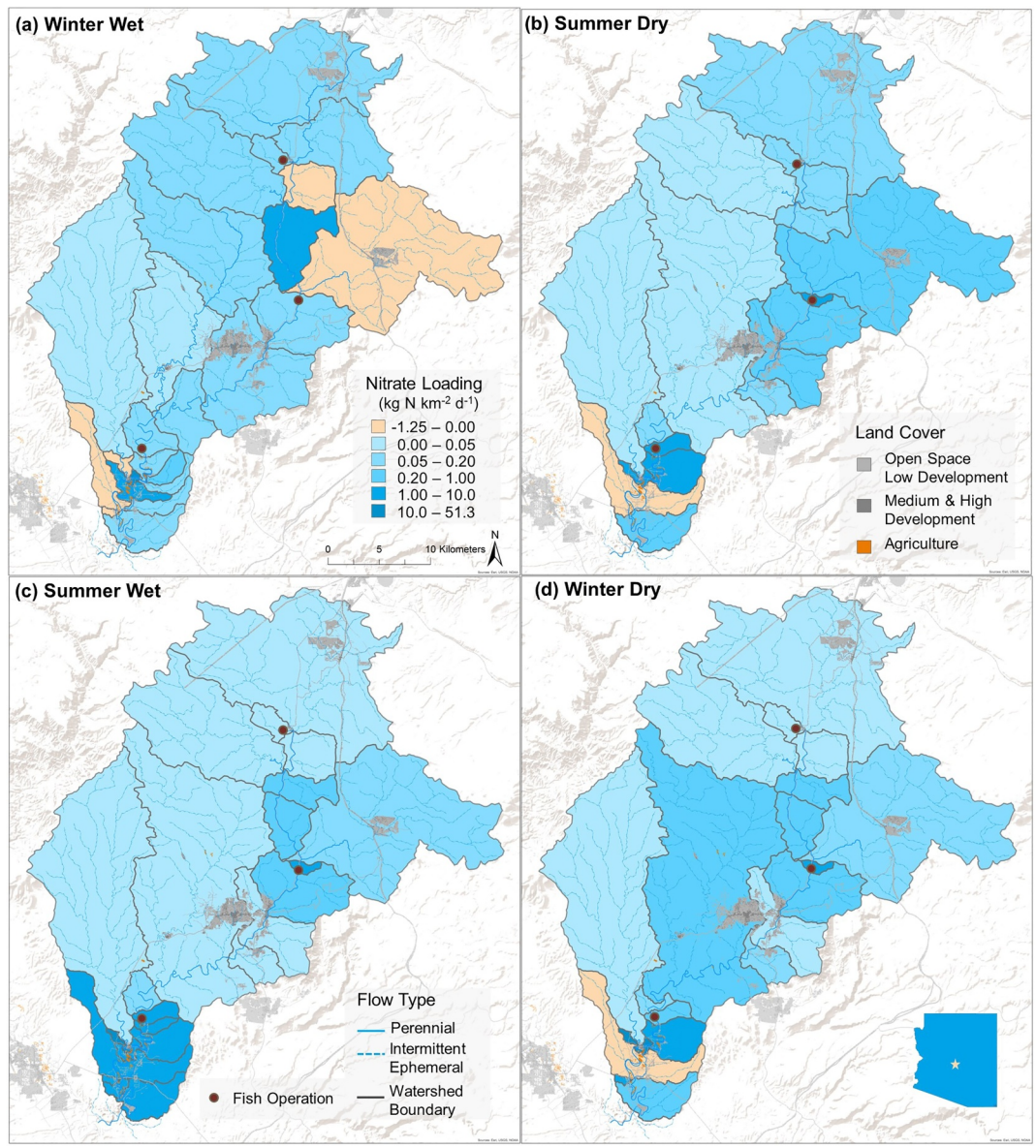

Figure 5. Modeled lateral NO_3^- loads to the stream for each subcatchment for the (a) winter wet, (b) summer dry, (c) summer wet, and (d) winter dry seasons. Subcatchments drain to stream reaches that are bounded by samples collected in the synoptic sampling campaigns. Fish operations include hatcheries and farms that were included as point sources in the model. Note the non-linear scale for the lateral NO_3^- loads and differences in subcatchment areas between seasons.

Table 4
Spearman Rank Correlations Coefficients Between the Lateral NO_3^- Loading and Proportion of the Subcatchment and 200-m Stream Buffer Area That is Wetlands, Agriculture, or Developed Land Cover

Area	Winter wet	Summer dry	Summer wet	Winter dry
Observations	19	16	17	16
Subcatchment				
Wetland	+0.23	+0.34	+0.40	+0.17
Agriculture	+0.37	+0.31	+0.56*	+0.19
Developed	+0.28	+0.50	+0.55*	+0.25
200-m Stream Buffer				
Wetland	+0.17	+0.32	+0.34	+0.30
Agriculture	+0.28	+0.49	+0.73*	+0.56*
Developed	+0.40	+0.60*	+0.53*	+0.44

Note. Asterisks denote a significant correlation (*$p < 0.05$).

land cover (median = 0%–7%) as did wetlands (median 0%–7%). Generally, correlations between land-cover type and lateral NO_3^- loading were more often detected, had higher correlation coefficients, and lower p-values when evaluated for the 200-m buffer area compared to the subcatchment area (Table 4). Evaluated at the subcatchment scale, lateral NO_3^- loading was positively correlated with agricultural cover only in the summer wet season. Evaluated at the 200-m buffer scale, lateral NO_3^- loading was positively correlated with agricultural cover in the summer wet and winter dry seasons. Evaluated at the subcatchment scale, lateral NO_3^- loading was positively correlated with developed area for only the summer wet season. Lateral NO_3^- loading was not correlated with wetland area for any of the seasons. Evaluated at the 200-m buffer scale, lateral NO_3^- loading was positively correlated with developed land area in both summer dry and summer wet seasons. In contrast to land cover, we found no consistent seasonal relationship between lateral NO_3^- loading and either modeled lateral water yield or measured stream discharge, width, water depth, or chemistry (Table S3 in Supporting Information S1).

4. Discussion

Our study of Oak Creek watershed addresses the crucial need to understand nitrogen dynamics and ecosystem functioning of dryland stream networks across seasons and along the fluvial network. We found that the pattern along the fluvial network in stream NO_3^- concentration and lateral NO_3^- loading was synchronous among three of the four seasons sampled. The winter wet season had more headwaters and tributaries with flowing surface water. This hydrologic connection facilitated lateral NO_3^- loads in these parts of the watershed while downstream sections had lower lateral NO_3^- loads that were not related to land cover. In contrast, the summer dry, summer wet, and winter dry seasons lacked surface water in the headwaters and many tributaries, but had consistently higher lateral NO_3^- loads in the lower section of the watershed. While our expectation was that seasons with higher precipitation and higher lateral NO_3^- loads might exceed in-stream NO_3^- uptake, we instead found high in-stream NO_3^- uptake maintained low stream NO_3^- concentration along the fluvial network and low NO_3^- export at the watershed outlet in all seasons (Table 5).

Table 5
Summary of the Major Findings of This Study Comparing the Seasonal Patterns of Hydrologic Connectivity, Lateral NO_3^- Load, and Stream NO_3^- Dynamics for the Headwater and Tributaries Region Versus the Lower Main Stem and Irrigation Ditches in Oak Creek

	Winter wet	Summer dry summer wet winter dry
Intermittent Headwaters & Tributaries		
Flowing surface water	Present	Absent
Land-stream connectivity	Higher	Lower
Lateral NO_3^- loading	Higher	Lower
Lower Main Stem and Irrigation Ditches		
Irrigation water demand	Lower	Higher
Land-stream connectivity	Lower	Higher
Lateral NO_3^- loading	Lower	Higher
Whole Stream Network		
Stream NO_3^- uptake	High	
Stream NO_3^- hydrologic loss	Low	
Stream NO_3^- concentration	Low	
Stream NO_3^- export	Low	

4.1. Seasonal Differences in Fluvial Network Patterns

Our investigation of Oak Creek's dryland stream network revealed distinct spatial patterns in lateral NO_3^- loading across seasons. The summer dry, summer wet, and winter dry seasons had lower overall discharge and a smaller proportion of the network maintaining flowing surface water compared to the winter wet season. The similarity in hydrologic variables across these three seasons appears to have consequences for stream chemistry and nitrogen cycling. We found NO_3^- and Cl^- concentrations as well as lateral NO_3^- loading were correlated among resampled sites and subcatchments in the summer dry, summer wet, and winter dry seasons. This consistency in the spatial pattern under baseflow conditions could be indicative of the importance of geomorphic control on hydro-nutrient dynamics, including the connection to surrounding land cover. At low flow, a greater proportion of the stream discharge is connected to lateral and hyporheic subsurface flowpaths, the chemistry of which is distinct from surface water. This finding is consistent with studies from Sycamore Creek, an intermittent stream in Arizona, where the geomorphic template exerts strong influence on nutrient patterns in the stream by controlling the exchange of shallow subsurface water and groundwater with surface water (Dent & Grimm, 1999; Dent et al., 2001; Dong et al., 2017). The high demand for irrigation water during these seasons may also contribute to the seasonal synchrony in nutrient concentration and lateral NO_3^- loading during periods of low flow. In contrast, the larger contributing area and lack of irrigation inputs during the winter wet season may signal a greater proportion of inputs coming from surface runoff derived from snowmelt and precipitation, particularly in the intermittent headwaters.

There were distinct fluvial network patterns in the stream NO_3^- and Cl^- concentrations between the lower and upper portion of Oak Creek watershed the summer dry, summer wet, and winter dry seasons compared to the winter wet season. In the lower section of the watershed, the higher Cl^- may be sourced from a combination from groundwater inputs, developed land cover, and agricultural activities. Groundwater tends to be higher in Cl^- than precipitation (Brooks & Lemon, 2007). Developed land cover and agricultural activities can contribute Cl^- from fertilizer application (Lowrance et al., 1985) and runoff from impervious surfaces (Kaushal et al., 2018; Walsh et al., 2005). In contrast, the winter wet season took place during a period of comparatively higher discharge from a combination of precipitation and snow melt. These additional water inputs may dilute the incoming Cl^- in combination with lower inputs during the cooler winter months.

The winter wet season also had a distinct spatial pattern in NO_3^- concentration and lateral NO_3^- loading compared to the three other seasons. This may be evidence of different dynamics in this wetter, cooler season. Snow melt and runoff may transport nitrogen pools that have accumulated during the preceding dry period to the headwaters and tributary that had flowing surface water only in this season (Meixner et al., 2007; Merbt et al., 2016). In addition, irrigation demand would be lower during this period given the low temperatures, leading to lower irrigation water-driven hydrologic connectivity between landscape sources of NO_3^- and the stream network. The winter wet season was the one campaign where lateral NO_3^- loading had no significant relationship with any of the land cover variables. While we hypothesized that the wetter seasons would have higher lateral NO_3^- loading, these findings indicate instead that the spatial pattern of lateral NO_3^- loading is different in the wetter winter season with high NO_3^- loading to the headwaters and tributaries that lacked surface water in other seasons. It is important to point out, however, that the contrasts between seasons in this particular study year are not necessarily predictive of all years, given the high interannual variability in both winter and summer precipitation. In particular, a relatively weak monsoon may have led longitudinal patterns in the summer wet season to more closely resemble those of the summer dry and winter dry seasons.

4.2. Drivers of Stream NO_3^- Load: Land Cover and In-Stream NO_3^- Demand

We found in-stream NO_3^- uptake and hydrologic losses from the stream removed >98% of lateral NO_3^- inputs by the time water reached the Oak Creek outlet across all seasons. This was the case despite high lateral NO_3^- loading from land to stream in parts of the watershed. In all seasons, overall stream NO_3^- concentration, flow-weighted concentration, and NO_3^- export in Oak Creek remained low. The majority of the removal (>81%) occurred through in-stream NO_3^- uptake. This finding confirms our hypothesis that stream NO_3^- uptake can attenuate most lateral NO_3^- load in streams that are highly nitrogen-limited even with higher hydrologic connectivity.

Our findings underscore the importance of in-stream NO_3^- uptake in regulating nitrogen dynamics in Oak Creek. The NO_3^- uptake capacity in this study is high relative to streams across the U.S. (Hall et al., 2009). The median

vertical uptake velocity for this study was 12.3 mm/min, and ranged from 5.5 to 18.0 mm/min. For comparison, Hall et al. (2009) compiled 69 measurements of NO_3^- uptake in U.S. streams and found a median vertical uptake velocity of 0.44 mm/min, nearly two orders of magnitude lower than our study, with a range from 0.024 to 17.9 mm/min. The high NO_3^- uptake in Oak Creek is consistent with other dryland streams (Grimm & Fisher, 1986; Martí et al., 1997; Schade et al., 2001). Streams in Arizona are generally nitrogen-limited given the high phosphorus availability from geologic sources (Grimm & Fisher, 1986). In addition, high light availability in streams leads to high potential for algal productivity in the presence of nutrients (Martí et al., 1997). This finding aligns with the observation that, while lateral NO_3^- loading may be influenced by land cover combined with irrigation practices, these signals are substantially modified by the high in-stream NO_3^- demand (Seybold & McGlynn, 2018).

In Oak Creek, the lower portion of the watershed exhibited the highest lateral NO_3^- loading. This area of the watershed is characterized by large horseshoe bends with some agricultural operations and residential development as well as two large irrigation ditches. This lower portion of the watershed was a large driver of the correlations between lateral NO_3^- loading and both agricultural and developed land use in the summer dry, summer wet, and winter dry seasons. In these three seasons, temperature is moderate to high, precipitation is low or episodic, and demand for irrigation is moderate to high. While we expected that the warmer and drier seasons would have lower lateral NO_3^- loading, our findings instead indicate that irrigation-water inputs and high hydraulic conductivity in the lower portion of the watershed sustain lateral NO_3^- loads from land to stream during periods with discharge conditions close to baseflow (Gardner & McGlynn, 2009; Soil Survey Staff, 2019).

The relationship between land cover and stream nitrogen load and concentration is well established across many ecosystems (Dodds & Oakes, 2006; Poor & McDonnell, 2007; von Schiller et al., 2008; Walsh et al., 2005). A common practice in modeling stream nitrogen dynamics is to estimate lateral nitrogen loads to the stream based on the land cover in the watershed (Preston et al., 2011). This approach in Oak Creek may be appropriate during periods with low precipitation and high irrigation; however, this assumption is likely less appropriate in seasons or areas where there is less hydrologic connection between nutrient sources and the stream. This conclusion is consistent with other studies demonstrating a seasonal or spatial disconnect between nitrogen sources and the streams draining the landscape (Compton et al., 2019; Helton et al., 2011; Yates et al., 2014).

While the amount of agricultural and developed land cover in Oak Creek was low, these areas were associated with higher lateral NO_3^- loads in some seasons. Even small amounts of these land cover types can have a disproportionate impact on streams (Walsh et al., 2005; Walsh & Webb, 2015). The relationships between land cover and stream NO_3^- loading were more often detected, had higher correlation coefficients, and lower p-values when evaluated for a 200-m buffer area around the stream than when calculated for the subcatchment area, indicating that land cover near the stream has a larger effect than more distal land use (Walsh & Webb, 2014). The subcatchment area generally had lower proportions of the relevant land cover classes compared to the 200-m buffer area (Table S2 in Supporting Information S1). These land-cover types are regularly associated with higher lateral nitrogen loads to streams and high flow-weighted nitrogen concentration in surface waters (Aguilera et al., 2012; Allan et al., 1997; Sobota et al., 2009).

Comparing lateral NO_3^- loading values from this study to the literature is a challenge because the values in this study represent lateral NO_3^- loading from the landscape to the stream and are distinct from the stream NO_3^- uptake. The most comparable estimates come from the incremental total nitrogen load produced by the SPARROW model that incorporates stream channel nitrogen retention through both uptake and loss to the hyporheic and groundwater zone (Schwarz et al., 2006). To compare, we converted our lateral NO_3^- loading to total nitrogen. Nitrate can be near 90% of total nitrogen in dryland streams during stormflow but is generally closer to 0%–10% at lower flows (Grimm, 1987). Conservatively assuming that NO_3^- accounts for 20% of the total nitrogen in Oak Creek, then lateral total nitrogen loading estimates range from 0.0005 to 254 kg N km^{-2} d^{-1} with a median of 1.05 kg N km^{-2} d^{-1}. The median for Oak Creek is near the mean reported for Spain (1.1 kg N km^{-2} d^{-1}) (Aguilera et al., 2012) and much of the US (range: 0.55–3.48 kg N km^{-2} d^{-1}) (Brown et al., 2011; Hoos & McMahon, 2009; Moore et al., 2011; Rebich et al., 2011; Wise & Johnson, 2011). High lateral NO_3^- loading (>6 kg N km^{-2} d^{-1}) identified in this study is also within the range of that reported for agriculturally intensive areas, including California's Central Valley (range: 0.008–795 kg N km^{-2} d^{-1}) (Saleh & Domagalski, 2015) and the Great Lakes basins (0.002–1,263 kg N km^{-2} d^{-1}) (Robertson & Saad, 2013). Just 15% of the observations from this study are within the same order of magnitude or less than that measured for the

dryland Orange River in South Africa (0.09 kg N km^{-2} d^{-1}) (Caraco & Cole, 2001) and below the low range for California (0.08 kg N km^{-2} d^{-1}) (Saleh & Domagalski, 2015). Thus, compared to other studies, Oak Creek features lateral NO_3^- loading that spans a range from very low to high nitrogen inputs.

4.3. Modeling Challenges Addressed and Remaining Limitations

Our model addresses several challenges in representing the spatial hydrological complexities of dryland stream networks. A flexible modeling approach was necessary to represent the variable discharge conditions including (a) varying the extent of flowing surface water in the drainage network, (b) irrigation ditch diversions, and (c) net gaining and net losing stream reaches. This last feature was particularly important, as representing discharge as a net process of inflows and outflows in the model allowed for lateral NO_3^- loads to flow from landscape to stream even in reaches that were net losing discharge. These features are critical to representing the hydrology of dryland stream networks, but may also be common in other climatic regions (Acuña et al., 2017; Stubbington et al., 2017; von Schiller et al., 2011). Thus, the concepts are applicable to other ecosystem types (Fitzhugh & Richter, 2004; Helton et al., 2011).

One of the critical challenges in measuring and modeling nitrogen dynamics in dryland stream networks is the extent of variable discharge conditions coupled with the crucial role that water availability plays for nitrogen cycling. A small minority of streams in Arizona have perennial flow and the majority have temporary surface flow in response to precipitation or seasonal water availability (Botter et al., 2021; Marshall et al., 2010). With discharge conditions varying between the two extremes of low or zero flow and high-discharge floods, mean conditions are unlikely to capture the nitrogen dynamics of the system. Therefore, we employed a seasonal investigation of the NO_3^- dynamics in Oak Creek to characterize the transport and uptake of the nutrient according to seasonal conditions in water availability and associated nitrogen cycling. Yet the conditions that prevailed during this 1-year study also are unlikely to reflect mean conditions in the region, given high interannual variability in precipitation. In other words, another year with low winter precipitation and a strong summer monsoon season might have looked different than the study year. Nevertheless, our approach incorporates flexibility to address seasonal and interannual hydrologic variability characteristic of drylands.

In addition to challenges addressed, our study has several limitations that should be acknowledged. The first limitation is that we conducted nine stream NO_3^- uptake experiments and applied a single median of these NO_3^- uptake measurements in the model regardless of season or site type. We took this approach for two reasons: (a) There was some temporal mismatch between the winter wet season campaign and the associated NO_3^- uptake experiments in the main channel (April) and tributaries (March) and (b) there were no detected statistical differences based on season, site type, or the background stream NO_3^- concentration. However, there was variability in the measurements and the lack of inclusion of this variability may be in part why the model produced negative lateral NO_3^- loading for some subcatchments and seasons. Negative lateral NO_3^- loads are produced when the in-stream NO_3^- uptake and NO_3^- loss through water loss to groundwater are not high enough to account for the measured decrease in stream NO_3^- export between two consecutive reaches. While accurate estimates of NO_3^- loss via water loss is beyond the scope of this analysis, assigning variable NO_3^- uptake rates across seasons or site types that are within the range of the high NO_3^- uptake rates measured would yield similar spatial patterns in lateral NO_3^- loads and overall network uptake. Indeed, initial model tests with a higher or lower NO_3^- uptake parameter revealed the NO_3^- delivered to the stream is still mostly consumed by in-stream demand. In streams where or times when hydrologic retention may make up a larger proportion of NO_3^- loss, an important area of future work includes integrating field and modeling approaches to better constrain NO_3^- hydrologic loss through both diversion and groundwater in dryland networks.

The second limitation is the low number of subcatchments that match between the winter wet season and the three other seasons. While the summer dry, summer wet, and winter dry seasons had 12–17 subcatchments that covered identical areas for each pairwise seasonal comparison, the winter wet season only had 6–7 subcatchments that covered identical areas for pairwise comparison with the three other seasons. The low number of matching subcatchments between the winter wet season and the three other seasons may limit the statistical power to detect correlations between lateral NO_3^- loads among seasons. We found that the pairwise correlations for the lateral NO_3^- loads between the summer dry, summer wet, and winter dry seasons were not detected when we limited the matching subcatchments to those that cover identical areas in the winter wet season. Therefore, the lack of a correlation between the lateral NO_3^- loads in the winter wet season compared to the other three seasons may be a

consequence of the low number of comparable subcatchments. However, this limitation is absent in other analyses including the correlation of NO_3^- and Cl^- concentrations between pairwise comparisons of the winter wet season to the three other seasons and the relationship between lateral NO_3^- loads and land cover. As a result, the number of observations available for these two analyses was similar to those used in pairwise comparisons for the three other seasons. In both analyses, the lack of detectable relationships is further evidence that the winter wet season had a distinct pattern of stream chemistry and connection to nitrogen sources along the fluvial network despite this limitation.

5. Conclusions

Oak Creek, a dryland stream network, exhibits seasonal and spatial variations in lateral NO_3^- loads and stream uptake. The variation in loads was driven in part by seasonal variability in precipitation inputs, evapotranspiration, and irrigation practices which affect the extent of the flowing stream network and discharge. Previous studies have found that diversions for irrigation water can facilitate hydrologic connections between the surrounding landscape and the stream in otherwise dry ecosytems (Alger et al., 2021). In addition, we found that land cover closer to the stream was more often positively correlated with lateral NO_3^- loads. Even when lateral NO_3^- loading was high, the high capacity for in-stream NO_3^- uptake in Oak Creek played a pivotal role in the nitrogen dynamics by maintaining low in-stream NO_3^- concentration. These findings challenge conventional approaches to modeling stream nitrogen dynamics based largely on land cover, as they may not fully capture the dynamics of dryland streams with seasonal hydrologic disconnects and high in-stream nitrogen demand. Taken together, our results indicate that managing the land use activities, including nutrient sources and irrigation practices, near the stream channel may be an effective strategy for managing nutrient fluxes to the stream.

This study advances our knowledge of drylands and contributes to the broader understanding of ecosystems, encompassing not only the 40% of Earth's landmass that is dryland but also the remaining 60% (Prăvălie, 2016), where similar complexities and challenges in nitrogen dynamics may exist. While the conditions exhibited by Oak Creek are especially pronounced in dryland settings, they are not exclusive to such regions. Many ecosystems, even those in more mesic climates, may exhibit similar hydrologic complexities and concommittant modification by biogeochemical processes. While much more common in dryland ecosystems, temporary streams are widespread throughout different climatic regions (Skoulikidis et al., 2017; Stubbington et al., 2017). Water diversions are also widespread for irrigation (Goodrich et al., 2018) and interbasin-transfers (Fitzhugh & Richter, 2004). In addition, while there is evidence that streams can become nitrogen-saturated due to large inputs from human activities (Earl et al., 2006), many streams remain nitrogen-limited (Andersen et al., 2006). In nitrogen-limited systems, landscape nitrogen loads can be heavily modified by the in-stream nitrogen demand. Taken together, the recognition and refinement of models capable of capturing both hydrologic context (season, extent of flowing network, and discharge) and biological controls will not only enhance our understanding of drylands but also contribute to the understanding of stream network biogeochemistry in other climatic regions. Moreover, the threat of climate change emphasizes the urgency of comprehending the ecological dynamics of dryland stream networks that will become increasingly common in a warmer and drier future (Leigh et al., 2015).

Data Availability Statement

The data and code for this analysis are available at https://doi.org/10.6073/pasta/68273eab165af073371b126d6d8c05f8 (Handler et al., 2024).

Acknowledgments
This research was funded by a Grant from School of Life Sciences Research and Training Initiatives at Arizona State University to A.M. Handler and in part by NSF Grants DEB-1457227 and EF-1442522 to NBG. Thank you to Cathy Kochert, Natalie Day, and Keeley Maxwell for assistance with analyses. Thank you to Nicholas Armijo, Corey Caulkins, Kody Landals, Jeremiah McGehee, Kathrine Kemmitt, Marina Lauck, Heather Fischer, Ryan Reynolds, Sophia Bonjour, Monica Palta, Lauren McPhillips, and Lindsey Pollard for help in the field and lab. Thank you to the Central Arizona Phoenix Long Term Ecological Research Program (NSF Grants DEB-2224662 and DEB-1637590) for additional support. The views expressed in this article are those of the authors and do not necessarily represent the views or policies of the U.S. Environmental Protection Agency. Any mention of trade names, products, or services does not imply an endorsement by the U. S. Government or the U.S. Environmental Protection Agency. The EPA does not endorse any commercial products, services, or enterprises.

References

Acuña, V., Hunter, M., & Ruhí, A. (2017). Managing temporary streams and rivers as unique rather than second-class ecosystems. *Biological Conservation*, *211*, 12–19. https://doi.org/10.1016/j.biocon.2016.12.025

Aguilera, R., Marcé, R., & Sabater, S. (2012). Linking in-stream nutrient flux to land use and inter-annual hydrological variability at the watershed scale. *Science of the Total Environment*, *440*, 72–81. https://doi.org/10.1016/j.scitotenv.2012.08.030

Alger, M., Lane, B. A., & Neilson, B. T. (2021). Combined influences of irrigation diversions and associated subsurface return flows on river temperature in a semi-arid region. *Hydrological Processes*, *35*(8), e14283. https://doi.org/10.1002/hyp.14283

Allan, J. D., Erickson, D. L., & Fay, J. (1997). The influence of catchment land use on stream integrity across multiple spatial scales. *Freshwater Biology*, *37*(1), 149–161. https://doi.org/10.1046/j.1365-2427.1997.d01-546.x

Andersen, H. E., Kronvang, B., Larsen, S. E., Hoffmann, C. C., Jensen, T. S., & Rasmussen, E. K. (2006). Climate-change impacts on hydrology and nutrients in a Danish lowland river basin. *Science of the Total Environment*, *365*(1), 223–237. https://doi.org/10.1016/j.scitotenv.2006.02.036

Arce, M. I., Sánchez-Montoya, M. d. M., Vidal-Abarca, M. R., Suárez, M. L., & Gómez, R. (2014). Implications of flow intermittency on sediment nitrogen availability and processing rates in a Mediterranean headwater stream. *Aquatic Sciences*, *76*(2), 173–186. https://doi.org/10.1007/s00027-013-0327-2

Belnap, J., Welter, J. R., Grimm, N. B., Barger, N. N., & Ludwig, J. A. (2005). Linkages between microbial and hydrologic processes in arid and semiarid watersheds. *Ecology*, *86*(2), 298–307. https://doi.org/10.1890/03-0567

Bernal, S., von Schiller, D., Sabater, F., & Martí, E. (2013). Hydrological extremes modulate nutrient dynamics in mediterranean climate streams across different spatial scales. *Hydrobiologia*, *719*(1), 31–42. https://doi.org/10.1007/s10750-012-1246-2

Bernhardt, E. S., Blaszczak, J. R., Ficken, C. D., Fork, M. L., Kaiser, K. E., & Seybold, E. C. (2017). Control points in ecosystems: Moving beyond the hot spot hot moment concept. *Ecosystems*, *20*(4), 665–682. https://doi.org/10.1007/s10021-016-0103-y

Botter, G., Vingiani, F., Senatore, A., Jensen, C., Weiler, M., McGuire, K., et al. (2021). Hierarchical climate-driven dynamics of the active channel length in temporary streams. *Scientific Reports*, *11*(1), 21503. https://doi.org/10.1038/s41598-021-00922-2

Brooks, P. D., & Lemon, M. M. (2007). Spatial variability in dissolved organic matter and inorganic nitrogen concentrations in a semiarid stream, San Pedro River, Arizona. *Journal of Geophysical Research*, *112*(3), 1–11. https://doi.org/10.1029/2006JG000262

Brown, J. B., Sprague, L. A., & Dupree, J. A. (2011). Nutrient sources and transport in the Missouri River Basin with emphasis of the effect of irrigation and reservoirs. *Journal of the American Water Resources Association*, *47*(5), 1034–1060. https://doi.org/10.1111/j.1752-1688.2011.00584.x

Caraco, N. F., & Cole, J. J. (2001). Human influence on nitrogen export: A comparison of mesic and xeric catchments. *Marine and Freshwater Research*, *52*(1), 119–125. https://doi.org/10.1111/j.1550-7408.2011.00547.x

Collins, S. L., Belnap, J., Grimm, N. B., Rudgers, J. A., Dahm, C. N., Odorico, P. D., et al. (2014). A multiscale, hierarchical model of pulse dynamics in arid-land ecosystems. *Annual Review of Ecology Evolution and Systematics*, *45*(1), 397–419. https://doi.org/10.1146/annurev-ecolsys-120213-091650

Compton, J. E., Goodwin, K. E., Sobota, D. J., & Lin, J. (2019). Seasonal disconnect between streamflow and retention shapes riverine nitrogen export in the Willamette river basin, Oregon. *Ecosystems*, *23*(1), 1–17. https://doi.org/10.1007/s10021-019-00383-9

Covino, T. P., McGlynn, B. L., & Baker, M. A. (2010). Separating physical and biological nutrient retention and quantifying uptake kinetics from ambient to saturation in successive mountain stream reaches. *Journal of Geophysical Research*, *115*(4), 1–17. https://doi.org/10.1029/2009JG001263

Dahm, C. N., & Molles, M. C. (1992). *Streams in semiarid regions as sensitive indicators of global climate change*. In S. G. Fisher & P. Firth (Eds.), (pp. 250–260). Springer-Verlag.

Day, T. J., & Day, T. T. (1977). Field procedures and evaluation of a slug dilution gauging method in mountain streams. *Journal of Hydrology*, *16*(2), 113–133. Retrieved from http://www.jstor.org/stable/43944411

Dent, C. L., & Grimm, N. B. (1999). Spatial heterogeneity of stream water nutrient concentrations over successional time. *Ecology*, *80*(7), 2283–2298. https://doi.org/10.1890/0012-9658(1999)080[2283:SHOSWN]2.0.CO;2

Dent, C. L., Grimm, N. B., & Fisher, S. G. (2001). Multiscale effects of surface–subsurface exchange on stream water nutrient concentrations. *Journal of the North American Benthological Society*, *20*(2), 162–181. https://doi.org/10.2307/1468313

Dewitz, J. (2014). National Land Cover Database (NLCD) 2011 land cover conterminous United States.

Dodds, W. K., & Oakes, R. M. (2006). Controls on nutrients across a Prairie stream watershed: Land use and riparian cover effects. *Environmental Management*, *37*(5), 634–646. https://doi.org/10.1007/s00267-004-0072-3

Dong, X., Ruhí, A., & Grimm, N. B. (2017). Evidence for self-organization in determining spatial patterns of stream nutrients, despite primacy of the geomorphic template. *Proceedings of the National Academy of Sciences*, *114*(24), E4744–E4752. https://doi.org/10.1073/pnas.1617571114

Earl, S. R., Valett, H. M., & Webster, J. R. (2006). Nitrogen saturation in stream ecosystems. *Ecology*, *87*(12), 3140–3151. https://doi.org/10.1890/0012-9658(2006)87[3140:NSISE]2.0.CO;2

Fischer, S. J., Grimm, N. B., Martí, E., Holmes, R. M. H., Jones, J. B., Fisher, S. G., & Jones, J. B. (1998). Material spiraling in stream corridors: A telecoping ecosystem model. *Ecosystems*, *1*, 19–34. https://doi.org/10.1007/s100219900003

Fitzhugh, T. W., & Richter, B. D. (2004). Quenching urban thirst: Growing cities and their impacts on freshwater ecosystems. *BioScience*, *54*(8), 741–754. https://doi.org/10.1641/0006-3568(2004)054[0741:Qutgca]2.0.Co;2

Galloway, J. N., Dentener, F. J., Capone, D. G., Boyer, E. W., Howarth, R. W., Seitzinger, S. P., et al. (2004). Nitrogen cycles: Past, present, and future. *Biogeochemistry*, *70*(2), 153–226. https://doi.org/10.1007/s10533-004-0370-0

Gardner, K. K., & McGlynn, B. L. (2009). Seasonality in spatial variability and influence of land use/land cover and watershed characteristics on stream water nitrate concentrations in a developing watershed in the Rocky Mountain West. *Water Resources Research*, *45*(8), 1–14. https://doi.org/10.1029/2008WR007029

Gómez-Gener, L., Siebers, A. R., Arce, M. I., Arnon, S., Bernal, S., Bolpagni, R., et al. (2021). Towards an improved understanding of biogeochemical processes across surface-groundwater interactions in intermittent rivers and ephemeral streams. *Earth-Science Reviews*, *220*, 103724. https://doi.org/10.1016/j.earscirev.2021.103724

Goodrich, D. C., Kepner, W. G., Levick, L. R., & Wigington Jr, P. J. (2018). Southwestern intermittent and ephemeral stream connectivity. *JAWRA Journal of the American Water Resources Association*, *54*(2), 400–422. https://doi.org/10.1111/1752-1688.12636

Grimm, N. B. (1987). Nitrogen dynamics during succession in a desert stream. *Ecology*, *68*(5), 1157–1170. https://doi.org/10.2307/1939200

Grimm, N. B., & Fisher, S. G. (1986). Nitrogen limitation in a Sonoran desert stream. *North American Benthological Society*, *5*(1), 2–15. https://doi.org/10.2307/1467743

Grimm, N. B., & Petrone, K. C. (1997). Nitrogen fixation in a desert stream ecosystem. *Biogeochemistry*, *1991*, 33–61.

Hall, R. O., Tank, J. L., Sobota, D. J., Mulholland, P. J., Jonathan, M., Brien, O., et al. (2009). Nitrate removal in stream ecosystems measured by total uptake 15 N addition experiments: Total uptake. *Limnology & Oceanography*, *54*(3), 653–665. https://doi.org/10.4319/lo.2009.54.3.0653

Handler, A. M., Grimm, N. B., & Helton, A. M. (2024). Stream nitrate concentrations and discharge, stream nitrate uptake, and results of stream network nitrate model to determine lateral nitrate load from land to stream in Oak Creek, Arizona, USA [Dataset]. https://doi.org/10.6073/pasta/68273eab165af073371b126d6d8c05f8

Helton, A. M., Poole, G. C., Meyer, J. L., Wollheim, W. M., Peterson, B. J., Mulholland, P. J., et al. (2011). Thinking outside the channel: Modeling nitrogen cycling in networked river ecosystems. *Frontiers in Ecology and the Environment*, *9*(4), 229–238. https://doi.org/10.1890/080211

Hill, R. W., & Walter, I. A. (2020). In B. R. Fath & S. E. Jorgensen (Eds.), *Irrigation: River flow impact* (2nd ed., pp. 165–170). CRC Press.

Hoos, A. B., & McMahon, G. (2009). Spatial analysis of instream nitrogen loads and factors controlling nitrogen delivery to streams in the southeastern United States using spatially referenced regression on watershed attributes (SPARROW) and regional classification framworks. *Hydrological Processes*, *23*(16), 2275–2294. https://doi.org/10.1002/hyp

Jencso, K. G., McGlynn, B. L., Gooseff, M. N., Wondzell, S. M., Bencala, K. E., & Marshall, L. A. (2009). Hydrologic connectivity between landscapes and streams: Transferring reach- and plot-scale understanding to the catchment scale. *Water Resources Research*, *45*(4), 1–16. https://doi.org/10.1029/2008WR007225

Kaushal, S. S., Likens, G. E., Pace, M. L., Utz, R. M., Haq, S., Gorman, J., & Grese, M. (2018). Freshwater salinization syndrome on a continental scale. *Proceedings of the National Academy of Sciences*, *115*(4), E574–E583. https://doi.org/10.1073/pnas.1711234115

Lange, J. (2005). Dynamics of transmission losses in a large arid stream channel. *Journal of Hydrology*, *306*(1), 112–126. https://doi.org/10.1016/j.jhydrol.2004.09.016

Leigh, C., Boulton, A. J., Courtwright, J. L., Fritz, K. M., May, C. L., Walker, R. H., & Datry, T. (2015). Ecological research and management of intermittent rivers: An historical review and future directions. *Freshwater Biology*, *61*(8), 1181–1199. https://doi.org/10.1111/fwb.12646

Leopold, L. B., & Maddock, T. (1953). The hydraulic geometry of stream channels and some physiograhpic implications.

Lowrance, R. R., Leonard, R. A., Asmussen, L. E., & Todd, R. L. (1985). Nutrient budgets for agricultural watersheds in the southeastern coastal plain. *Ecology*, *66*(1), 287–296. https://doi.org/10.2307/1941330

Marshall, R. M., Robles, M. D., Majka, D. R., & Haney, J. A. (2010). Sustainable water management in the Southwestern United States: Reality or Rhetoric? *PLoS One*, *5*(7), e11687. https://doi.org/10.1371/journal.pone.0011687

Martí, E., Grimm, N. B., & Fisher, S. G. (1997). Pre- and post-flood retention efficiency of nitrogen in a Sonoran Desert stream. *Journal of the North American Benthological Society*, *16*(4), 805–819. https://doi.org/10.2307/1468173

Martí, E., & Sabater, F. (1996). High variability in temporal and spatial nutrient retention in mediterranean streams. *Ecology*, *77*(3), 854–869. https://doi.org/10.2307/2265506

Meixner, T., Huth, A. K., Brooks, P. D., Conklin, M. H., Grimm, N. B., Bales, R. C., et al. (2007). Influence of shifting flow paths on nitrogen concentrations during monsoon floods, San Pedro River, Arizona. *Journal of Geophysical Research*, *112*(3), 1–11. https://doi.org/10.1029/2006JG000266

Merbt, S. N., Proia, L., Prosser, J. I., Martí, E., Casamayor, E. O., & von Schiller, D. (2016). Stream drying drives microbial ammonia oxidation and first-flush nitrate export. *Ecology*, *97*(9), 2192–2198. https://doi.org/10.1002/ecy.1486

Moore, R. B., Johnston, C. M., Smith, R. A., & Milstead, B. (2011). Sources and delivery of nutrients to the receiving water in the Northeastern and Mid-Atlantic regions of the United States. *Journal of the American Water Resources Association*, *47*(5), 965–990. https://doi.org/10.1111/j.1752-1688.2011.00582.x

Mulholland, P. J., Helton, A. M., Poole, G. C., Hall, R. O., Hamilton, S. K., Peterson, B. J., et al. (2008). Supplementary information: Stream denitrification across biomes and its response to anthropogenic nitrate loading. *Nature*, *254*. https://doi.org/10.1038/nature06686

Newbold, J. D., Elwood, J. W., O'Neill, R. V., & Winkle, W. V. (1981). Measuring nutrient spiralling in streams. *Canadian Journal of Fisheries and Aquatic Sciences*, *38*(7), 860–863. https://doi.org/10.1139/f81-114

Noy-Meir, I. (1973). Desert ecosystems: Environment and producers. *Annual Review of Ecology and Systematics*, *4*(1), 25–51. https://doi.org/10.1146/annurev.es.04.110173.000325

Oak Creek Watershed Council. (2012). Improvement plan for the Oak Creek Watershed, Arizona.

O'Brien, J. M., Dodds, W. K., Wilson, K. C., Murdock, J. N., & Eichmiller, J. (2007). The saturation of N cycling in central plains streams: 15N experiments across a broad gradient of nitrate concentrations. *Biogeochemistry*, *84*(1), 31–49. https://doi.org/10.1007/s10533-007-9073-7

Poor, C. J., & McDonnell, J. J. (2007). The effects of land use on stream nitrate dynamics. *Journal of Hydrology*, *332*(1), 54–68. https://doi.org/10.1016/j.jhydrol.2006.06.022

Prăvălie, R. (2016). Drylands extent and environmental issues. A global approach. *Earth-Science Reviews*, *161*, 259–278. https://doi.org/10.1016/j.earscirev.2016.08.003

Preston, S. D., Alexander, R. B., Schwarz, G. E., & Crawford, C. G. (2011). Factors affecting stream nutrient loads: A synthesis of regional SPARROW model results for the continental United States. *Journal of the American Water Resources Association*, *47*(5), 891–915. https://doi.org/10.1111/j.1752-1688.2011.00577.x

R Core Team. (2023). *R: A language and environment for statistical computing*. R Foundation for Statistical Computing. Retrieved from https://www.R-project.org/

Rebich, R. A., Houston, N. A., Mize, S. V., Pearson, D. K., Ging, P. B., & Hornig, C. E. (2011). Sources and delivery of nutrient to the Northwestern Gulf of Mexico from stream in the South-Central United States. *Journal of the American Water Resources Association*, *47*(5), 1061–1086. https://doi.org/10.1111/j.1752-1688.2011.00583.x

Ren, J., Hanan, E., D'Odorico, P., Tague, C., Schimel, J., & Homyak, P. (2023). Dryland watersheds in flux: How nitrogen deposition and changing precipitation regimes shape nitrogen export.

Robertson, D. M., & Saad, D. A. (2013). Nutrient inputs to the Laurentian Great Lakes by source and watershed estimated using SPARROW watershed models. *Journal of the American Water Resources Association*, *49*(3), 725–734. https://doi.org/10.1111/jawr.12060

Saleh, D., & Domagalski, J. (2015). SPARROW modeling of nitrogen sources and transport in rivers and stream of California and adjacent states, US. *Journal of the American Water Resources Association*, *51*(6), 1483–1507. https://doi.org/10.1111/1752-1688.12325

Schade, J. D., Fisher, S. G., Grimm, N. B., & Seddon, J. (2001). The influence of a riparian shrub on nitrogen cycling in a Sonoran Desert stream. *Ecology*, *82*(12), 3363–3376. https://doi.org/10.1890/0012-9658(2001)082[3363:tioars]2.0.co;2

Schwarz, G. E., Hoos, A. B., Alexander, R. B., & Smith, R. A. (2006). The SPARROW surface water-quality model: Theory, application and user documentation. In *U.S. Geological survey techniques and methods* (Vol. 6). U.S. Geological Survey.

Seybold, E., & McGlynn, B. (2018). Hydrologic and biogeochemical drivers of dissolved organic carbon and nitrate uptake in a headwater stream network. *Biogeochemistry*, *138*(1), 23–48. https://doi.org/10.1007/s10533-018-0426-1

Skoulikidis, N. T., Sabater, S., Datry, T., Morais, M. M., Buffagni, A., Dörflinger, G., et al. (2017). Non-perennial Mediterranean rivers in Europe: Status, pressures, and challenges for research and management. *Science of the Total Environment*, *577*, 1–18. https://doi.org/10.1016/j.scitotenv.2016.10.147

Sobota, D. J., Harrison, J. A., & Dahlgren, R. A. (2009). Influences of climate, hydrology, and land use on input and export of nitrogen in California watersheds. *Biogeochemistry*, *94*(1), 43–62. https://doi.org/10.1007/s10533-009-9307-y

Soil Survey Staff. (2019). *Web Soil Survey (STATSGO)*. Retrieved from http://websoilsurvey.nrcs.usda.gov/

Stieglitz, M., Shaman, J., McNamara, J. P., Engel, V., Shanley, J., & Kling, G. W. (2003). An approach to understanding hydrologic connectivity on the hillslope and the implications for nutrient transport. *Global Biogeochemical Cycles*, *17*(4), 1–15. https://doi.org/10.1029/2003GB002041

Stubbington, R., England, J., Wood, P. J., & Sefton, C. E. M. (2017). Temporary streams in temperate zones: Recognizing, monitoring and restoring transitional aquatic-terrestrial ecosystems. *WIREs Water*, *4*(4), e1223. https://doi.org/10.1002/wat2.1223

Valett, H. M., Fisher, S. G., Grimm, N. B., & Camill, P. (1994). Vertical hydrologic exchange and ecological stability of a desert stream ecosystem. *Ecology*, *75*(2), 548–560. https://doi.org/10.2307/1939557

von Schiller, D., Acuña, V., Graeber, D., Martí, E., Ribot, M., Sabater, S., et al. (2011). Contraction, fragmentation and expansion dynamics determine nutrient availability in a Mediterranean forest stream. *Aquatic Sciences*, *73*(4), 485–497. https://doi.org/10.1007/s00027-011-0195-6

von Schiller, D., Bernal, S., Dahm, C. N., & Martí, E. (2017). Nutrient and organic matter dynamics in intermittent rivers and ephemeral streams. In T. Datry, N. Bonada, & A. Boulton (Eds.), *Intermitted rivers and ephemeral streams, ecology and management* (pp. 135–160). Academic Press.

von Schiller, D., Martí, E., Riera, J. L., Ribot, M., Marks, J. C., & Sabater, F. (2008). Influence of land use on stream ecosystem function in a Mediterranean catchment. *Freshwater Biology*, *53*(12), 2600–2612. https://doi.org/10.1111/j.1365-2427.2008.02059.x

Walsh, C. J., Roy, A. H., Feminella, J. W., Cottingham, P. D., Groffman, P. M., & Morgan, R. P. (2005). The urban stream syndrome: Current knowledge and the search for a cure. *Journal of the North American Benthological Society*, *24*(3), 706–723. https://doi.org/10.1899/04-028.1

Walsh, C. J., & Webb, J. A. (2014). Spatial weighting of land use and temporal weighting of antecedent discharge improves prediction of stream condition. *Landscape Ecology*, *29*(7), 1171–1185. https://doi.org/10.1007/s10980-014-0050-y

Walsh, C. J., & Webb, J. A. (2015). Interactive effects of urban stormwater drainage, land clearance, and flow regime on stream macroinvertebrate assemblages across a large metropolitan region. *Freshwater Science*, *35*(1), 324–339. https://doi.org/10.1086/685105

Welter, J. R., Fisher, S. G., & Grimm, N. B. (2005). Nitrogen transport and retention in an arid land watershed: Influence of storm characteristics on terrestrial-aquatic linkages. *Biogeochemistry*, *76*(3), 421–440. https://doi.org/10.1007/sl0533-005-6997-7

Wise, D. R., & Johnson, H. M. (2011). Surface-water nutrient conditions and sources in the United States Pacific Northwest. *Journal of the American Water Resources Association*, *47*(5), 1110–1135. https://doi.org/10.1111/j.1752-1688.2011.00580.x

Wollheim, W. M., Bernal, S., Burns, D. A., Czuba, J. A., Driscoll, C. T., Hansen, A. T., & Wohl, E. E. (2018). River network saturation hypothesis: Factors influencing the balance of biogeochemical supply and demand of river networks. *Biogeochemistry*, 1–19. https://doi.org/10.1007/s10533-018-0488-0

Wollheim, W. M., Vörösmarty, C. J., Peterson, B. J., Seitzinger, S. P., & Hopkinson, C. S. (2006). Relationship between river size and nutrient removal. *Geophysical Research Letters*, *33*(6), 2–5. https://doi.org/10.1029/2006GL025845

Yates, A. G., Brua, R. B., Corriveau, J., Culp, J. M., & Chambers, P. A. (2014). Seasonally driven variation in spatial relationships between agricultural land use and in-stream nutrient concentrations. *River Research and Applications*, *30*(4), 476–493. https://doi.org/10.1002/rra.2646